SAND2011-2242C

Hydrogen-Assisted Deformation and Fracture of Austenitic Stainless Steels

C. San Marchi[1,*], B.P. Somerday[2], H.F. Jackson[3]

[1,2,3]Sanda National Laboratories
7011 East Ave, Livermore CA 94551 USA
[1]cwsanma@sandia.gov
[2]bpsomer@sandia.gov
[3]hfjacks@sandia.gov

ABSTRACT

The role of hydrogen on deformation and fracture has been discussed at great length in the literature. However, detailed characterization of the effects of hydrogen on deformation and fracture in real engineering materials is relatively limited. In this work, transmission electron microscopy is used to characterize deformation in two austenitic stainless steels: metastable type 316L and stable 21-6-9. Hydrogen suppresses deformation twinning in these materials and promotes the formation of strain-induced ε-martensite. Although not directly observed, the theoretical framework of hydrogen enhanced localized plasticity is used to rationalize the hydrogen-dislocation interactions in materials that deform by twinning and explain the observed fracture morphology.

Keywords: austenitic stainless steels, hydrogen-assisted fracture, hydrogen-enhanced localized plasticity

1. Introduction

There are many theories that attempt to describe hydrogen-assisted fracture in metals [1]. Several of these invoke the role of hydrogen in localizing deformation. Observations of increased dislocation mobility are used as evidence of hydrogen enhanced localized plasticity (HELP) and hydrogen-induced softening. However, as pointed out by Birnbaum and co-authors, enhanced dislocation velocities and softening are greatest at low stress [2, 3]. Modeling of the dislocation interactions in the presence of hydrogen show that hydrogen can effectively shield the stress centers associated with dislocation, allowing dislocations to come closer together [4]. On the other hand, *ab initio* calculations show that hydrogen can reduce the Peierls stress [5], which would also increase dislocation mobility, although again primarily at low stress. If the experimental data on nickel [2, 3] is any indication, at the high stresses associated with fracture, hydrogen may have little (if any) impact on dislocation mobility and softening.

It is important to recognize that austenitic stainless steels generally have low stacking fault energy (SFE), resulting in deformation that is governed by the characteristics of extended dislocations. For example, at high stress (such as those associated with fracture), deformation in austenitic stainless steels occurs by deformation twinning [6-8]. Descriptions of the effects of hydrogen on deformation in austenitic stainless steel must, at least, acknowledge the appropriate deformation modes. In this brief report, deformation microstructures of two austenitic stainless steels are examined in both the non-charged and hydrogen-precharged condition. The effects of hydrogen on these deformation microstructures are described and interpreted in the framework of hydrogen-enhanced localized plasticity. The role of deformation on hydrogen-assisted fracture is also briefly discussed.

2. Materials and Experimental Procedures

*Corresponding author

Two austenitic stainless steels are considered in this report: AISI type 316L and ASTM XM-10, the latter is commonly referred to in the literature by its nominal composition: 21Cr-6Ni-9Mn or simply 21-6-9. The composition of the two alloys is given in Table 1. Both alloys were obtained in the form of annealed wrought bar. In the as-received condition, the alloys had a uniform microstructure, free of magnetic phases (ferrite and α'-martensite).

Uniaxial tensile tests were performed on both alloys in the as-machined condition and after thermal precharging with hydrogen. Thermal precharging can be used to produce a nominally uniform hydrogen composition through the thickness of austenitic stainless steel test specimens. The diffusivity of hydrogen in this class of materials is sufficiently low that the hydrogen remains in the material over long periods so that mechanical testing can be performed in laboratory air without significant loss of hydrogen. Round tensile specimens (ASTM E8 subsized) with a gauge diameter of approximately 4 mm were thermally precharged following the same procedures described elsewhere [9, 10]: namely, immersion in gaseous hydrogen at pressure of 138 MPa and temperature of 573 K for a minimum of two weeks. These conditions result in uniform saturation with 140 wt ppm hydrogen (~0.7 at%).

The tensile testing was conducted at a strain rate of approximately 1.5×10^{-3} s^{-1} following procedures described elsewhere [9-11]. Testing was performed at room temperature in air and at 223 K in an environmental chamber using evaporated liquid nitrogen for regulating temperature. Replicate specimens tested for each condition. The following mechanical properties were determined: 0.2% offset yield strength (S_y), ultimate strength (S_u, maximum engineering stress), uniform elongation (El_u, engineering strain at maximum load), elongation at fracture (El_t), and reduction of area (RA).

In the context of this study, the room temperature data is primarily for reference and comparison to previous testing of similar alloys [9, 10, 12]. Deformation microstructures were characterized only for the specimens tested at 223 K. Fracture surfaces of the broken tensile specimens were examined by SEM. Subsequently, sections were extracted from broken tensile specimens at three locations: (i) just beneath the fracture surface, (ii) in the uniformly deformed gauge section and (iii) in the non-deformed grip sections (threaded ends of specimens). Foils for transmission electron microscopy (TEM) were then prepared from these samples with the plane of the foil perpendicular to the tensile axis. Selected-area electron diffraction (SAED) was employed to identify the deformation structures and distribution of strain-induced phase transformations.

Table 1. Compositions (wt%) of the austenitic stainless steels used in this study.

ID	Alloy	Fe	Cr	Ni	Mn	Mo	N	C	Si	S	P
J	316L	Bal	16.34	10.15	1.72	2.05	0.062	0.025	0.536	0.025	0.027
Z	21-6-9	Bal	20.45	6.15	9.55	—	0.265	0.033	0.52	0.0013	0.018

3. Results

In general, nickel-containing austenitic stainless steels are ductile at room temperature and maintain their ductility and toughness to cryogenic temperatures. The elongation and reduction of area are essentially the same at room temperature and at temperature of 223 K for each alloy as shown in Table 2. Although both materials were acquired as annealed, the measured yield strength shows that neither alloy is in the fully annealed condition. With precharged hydrogen, the ductility of both alloys was reduced; in particular, the reduction of area was lowered by 40 to 50% consistent with previous reports for type 316 stainless steels [9, 12] and for 21-6-9 [10]. This reduction is significantly greater at the lower temperature, also consistent with previous reports on metastable austenitic stainless steels [11, 12]. The flow stress, however, is greater with the addition of hydrogen, as typically observed for austenitic stainless steels with high concentrations of hydrogen [9, 10, 12]. One exception is the type 316L alloy when tested at temperature of 223 K: the ultimate strength is reduced with internal hydrogen compared to without hydrogen, although the ultimate strength at temperature of 223 K remains greater than the ultimate strength at room temperature.

In the undeformed materials, the microstructures are relatively free of dislocations, although dislocation structures (e.g., tangles, dislocation pile-ups, etc.) were observed in some grains. Deformation twinning represents the primary deformation mode for these alloys at the investigated strains in the absence of hydrogen (Figure 1a and Figure 2). SAED confirms the presence of ε-martensite and α'-martensite in the type 316L alloy and the lack of ε-martensite and α'-martensite in the 21-6-9 alloy (Figures 1 and 2), as expected based on magnetic measurements and relative stability of these two alloys. In Figure 1a, the SAED pattern of the non-charged type 316L does not show strain-induced phase transformations; although, in general, strain-induced martensite is observed in this alloy. An SAED pattern without martensite was chosen to emphasize that the primary deformation mode at high stress in type 316 alloys is deformation twinning. The stresses and strains in the specimens from the uniformly deformed gauge section are characterized by the ultimate strength and uniform elongation, respectively, that is strains on the order of 30 to 40% and stresses of greater than 600 MPa for both materials. The stresses and strains in the specimens from necked regions are clearly much higher; however, qualitatively the deformation structures are similar to those observed in the uniformly deformed gauge section except with greater amounts of strain-induced martensites.

In this study, an enhancement in localized deformation due to hydrogen could not be resolved due to the high level of localized deformation that intrinsically occurs in these alloys (deformation twinning) and the large strains associated with these investigations. However, there were distinct differences in the character of deformation of these alloys with the addition of hydrogen. In both alloys, hydrogen appears to have suppressed deformation twinning and promoted the formation of ε-martensite (Figure 1b and Figure 3). In type 316 alloys, α'-martensite nucleates at the intersection of bands of ε-martensite (and may also nucleate homogeneously [13]); however, α'-martensite was not observed in the 21-6-9.

Table 2. Tensile properties of the austenitic stainless steels used in this study at room temperature (293 K) and at temperature of 223 K, both without hydrogen (non-charged) and with internal hydrogen (precharged).

Alloy	Test temperature	Condition	S_y (MPa)	S_u (MPa)	El_u (%)	El_t (%)	RA (%)
J 316L	293 K	non-charged	343	684	47	70	82
		precharged	414	744	44	54	42
	223 K	non-charged	434	930	47	66	79
		precharged	478	846	26	26	26
Z 21-6-9	293 K	non-charged	539	881	38	61	79
		precharged	669	957	38	55	50
	223 K	non-charged	698	1073	39	61	79
		precharged	784	1178	33	33	26

4. Discussion

The type 316L that was used in this investigation contains relatively low nickel content (10.15%) and relatively high nitrogen (0.062%) for this designation of alloy. The 21-6-9 is distinguished from type 316L by significantly lower nickel content (6.15%) and higher nitrogen content (0.265%) as well as high manganese content. The high nitrogen content provides additional strengthening to the 21-6-9 compared to type 316L and also improves the microstructural stability of 21-6-9 with respect to the formation of martensite [14]. Type 316L alloys are generally considered metastable, as they generally form α'-martensite when deformed at room temperature (or lower temperature), while 21-6-9 is considered stable and generally will not form martensite even when deformed at subambient temperature. The detailed microscopy presented here corroborates these general expectations for these classes of alloys. The unique observation here is that ε-martensite is promoted in a stable austenitic stainless steel; previous work reported hydrogen-enhanced formation of ε-martensite during

deformation of type 304 and 316 alloys. Although ε-martensite forms readily in type 316 alloys in the absence of hydrogen [15], the authors are unaware of previous reports of ε-martensite induced by applied stress/strain in 21-6-9, with or without hydrogen.

Deformation characteristics

For type 316 alloys, previous studies has been shown that deformation twinning is dominant at stresses greater than about 600 MPa [7, 8]. A similar conclusion can be drawn from the observations made in this investigation: deformation becomes highly localized on {111} slip planes in type 316 alloys at elevated stress. It is not surprising that the same features are apparent in the 21-6-9. Muellner et al. found that higher nitrogen content enhanced localized deformation, in particular deformation twinning, in type 316 alloys, which was attributed to nitrogen lowering stacking fault energy (SFE) [6]. Lower nickel content (as in 21-6-9) will also lower SFE [14]. Byun developed a simple dislocation model showing that the separation between extended (partial) dislocations becomes essentially unstable at high stress [16], suggesting that stacking faults will extend to grain boundaries and promote twin-dominated deformation. Since separation of extended dislocations is related to SFE [17], Byun's model shows that twin-dominated deformation is enhanced at low SFE. Since SFE decreases as temperature is lowered [13], localized deformation of this sort is also enhanced at low temperature [7]. Localization of deformation or planar slip, however, does not necessarily provide an explanation for lower ductility and toughness. Alloys that deform primarily by planar deformation (twinning) often show excellent ductility and toughness in the absence of hydrogen, as for 21-6-9 and type 316 alloys.

The role of hydrogen in materials that specifically deform by twinning has not been described in the literature. Hydrogen, however, has been shown to stabilize edge dislocations both experimentally [18] and theoretically [5, 19] in model systems. Hydrogen is believed to lower the energy of edge dislocations, essentially stabilizing the edge configuration of dislocations. Since only screw dislocations can cross slip, hydrogen effectively promotes planar slip, a form of localized deformation [5, 18, 19]. In austenitic stainless steels, where extended dislocations are important, a similar process is expected, the difference being that extended dislocation must recombine (as well as being of screw character) prior to cross slipping. Therefore, in order to cross slip in the presence of hydrogen, extended dislocations must overcome the energy associated with separation as well as the accommodate the higher energy configuration of the screw orientation. Since the separation of extended dislocations depends on SFE, the energy required for cross slip will be greater for materials (and environments) with lower SFE. For these reasons, planar slip is particularly enhanced in low SFE materials in the presence of hydrogen, such as austenitic stainless steels.

Prior theoretical work and environmental TEM studies has emphasized the role of hydrogen on stress-shielding dislocations and enhancing dislocation mobility [2-4, 20]. This prior body of work has generally considered slip as the primary deformation mode. The discussion above, however, shows that deformation in these austenitic stainless steels is dominated by extended dislocations and deformation twinning, perhaps suggesting a subtler role for hydrogen. For example, strain-induced ε-martensite does not normally form in 21-6-9, although when hydrogen is present this strain-induced phase transformation is promoted. Similar observations are made for type 316L, suggesting a fundamental character to this transition from deformation twins to ε-martensite. Indeed, deformation by twinning and the formation of strain-induced ε-martensite occur by similar processes. Deformation twins are formed when stacking faults on adjacent planes overlap producing a stacking arrangement of ABC-B-A-C-B, where the dashes proceed the faults. In contrast, ε-martensite is formed when stacking faults overlap on every other plane producing a stacking arrangement of ABC-BC-BC. Thus, hydrogen influences the fundamental deformation processes in austenitic stainless steels by affecting the arrangement of extended dislocations. While certainly an interesting observation, it remains unclear whether the strain-induced ε-martensite is particularly important to the fracture process in comparison to deformation twinning, since the structure of these defects is very similar in nature. Moreover, as mentioned above, planar slip by itself does not explain lower ductility and toughness.

One of the consequences of localized deformation is that dislocations will pile-up at obstacles. This will be true of extended dislocations as well, as applied stress provides the energy to recombine extended dislocations. Consider, for example, an annealing twin boundary (which are typically on the order of the grain size) that acts as an obstacle to planar slip. If planar slip is strongly enforced as in the austenitic stainless steels particularly in the presence of hydrogen, deformation will be characterized by parallel slip planes that impinge on the large annealing twin boundary, producing stress uniformly distributed across the boundary. In addition, the stresses around pile-ups could conceivably be higher in the presence of hydrogen, since higher energy is needed to promote the cross slip that relaxes the stresses associated with the pile-up. Indeed, Chateau et al. has shown that hydrogen enhances stresses particularly on symmetric slip planes in austenitic stainless steels [21], which is precisely the twin boundary. In short, deformation induces high stress on large annealing twin boundaries in austenitic stainless steels and this stress is magnified in the presence of hydrogen. This stress will likely be related to SFE, because, as described above, the energy necessary to locally relax stress by cross slip depends directly on SFE. Although other microstructural features participate in deformation and fracture, annealing twin boundaries can be susceptible to hydrogen-assisted fracture.

Fracture characteristics

The fracture morphology observed on the broken tensile specimens can be related to the descriptions above of deformation. Both alloys are ductile at room temperature and at temperature of 223 K in the absence of hydrogen. Relatively, flat fracture features are apparent on the fracture surfaces of both alloys when tested in the hydrogen-precharged condition at temperature of 223 K (Figure 4). Flat fracture "facets" of this type have been identified as annealing twin boundaries in austenitic stainless steels [22-24]. Similar fracture features have been observed in Cr-Mn austenitic stainless steels in the absence of hydrogen, and attributed to enhanced slip planarity at low temperature [25, 26]. The Cr-Mn austenitic stainless steels have particularly low stacking fault energy, resulting in deformation that is particularly planar [26]. In other words, the deformation and fracture morphologies that are observed for type 316L and 21-6-9 at low temperature in the presence of hydrogen are not unique to hydrogen-assisted fracture. Hydrogen enhances intrinsic localization mechanisms sufficiently to expose twin boundary fracture, primarily by stabilizing edge dislocations and enhancing planar slip.

Fracture of twin boundaries provides a useful illustration of the link between deformation and fracture; however, this fracture morphology has only been observed under a limited set of conditions for nickel-containing austenitic stainless steels. In particular, twin boundary fracture is observed for alloys with relatively low nickel content and at subambient temperature [22-24], i.e., conditions that particularly enhance planarity of slip. Although twin boundary fracture is not observed at room temperature in the two tested alloys, hydrogen-enhanced slip planarity remains active. In these and other austenitic stainless steels there is evidence of hydrogen-enhanced planar slip without twin boundary fracture [27-29]. In other words, the underlying mechanism of hydrogen-enhanced planar slip appears to be universal and damage can take many forms, evolving at other microstructural features. It has been suggested, for example, that enhanced planar slip causes void nucleation at the intersection of slip bands [30, 31], or voids may nucleate at inclusions as commonly observed for ductile metals.

5. Summary

It is well known that low SFE generally correlates with enhanced susceptibility to stress corrosion cracking and hydrogen embrittlement [32]. The description above shows that SFE is important to understanding hydrogen's role on enforcing planar slip modes in the examined austenitic stainless steels and more generally in materials that deform by twinning. Factors that the increase SFE are likely to improve resistance to hydrogen-assisted fracture. Nickel alloying content, for example, has a particularly strong effect on SFE and correspondingly on resistance to hydrogen-assisted fracture [9,

12]. The effects of temperature on hydrogen-assisted fracture can also be understood based on SFE. In these alloys with relatively low SFE, hydrogen suppresses deformation twinning and enhances the formation of strain-induced ε-martensite. The importance of this observation is not clear; although it is speculated that it has no significant effect on hydrogen-assisted fracture since deformation twins and strain-induced ε-martensite differ only in the arrangement of stacking faults.

Acknowledgments

The authors gratefully acknowledge the microscopy of Tom Headley and Nancy Yang at Sandia. Sandia National Laboratories is a multi-program laboratory managed and operated by Sandia Corporation, a wholly owned subsidiary of Lockheed Martin Corporation, for the U.S. Department of Energy's National Nuclear Security Administration under contract DE-AC04-94AL85000.

References

[1] S. P. Lynch, Corrosion 2007, Nashville TN, NACE International, paper no. 07493.
[2] H. K. Birnbaum, P. Sofronis, Mater Sci Eng A176 (1994) 191.
[3] H. K. Birnbaum, I. M. Robertson, P. Sofronis, D. Teter, in: Magnin T, (Ed.), Corrosion-Deformation Interactions, Woodhead Publishing Limited, Cambridge, 1997, pp. 172.
[4] P. Sofronis, H. K. Birnbaum, J Mech Phys Solids 43 (1995) 49.
[5] G. Lu, D. Orlikowski, I. Park, O. Politano, E. Kaxiras, Phys Rev B 65 (2002) 064102.
[6] P. Muellner, C. Solenthaler, P. Uggowitzer, M. O. Speidel, Mater Sci Eng A164 (1993) 164.
[7] T. S. Byun, N. Hashimoto, K. Farrell, Acta Mater 52 (2004) 3889.
[8] T. S. Byun, N. Hashimoto, K. Farrell, J Nucl Mater 351 (2006) 303.
[9] C. San Marchi, B. P. Somerday, X. Tang, G. H. Schiroky, Int J Hydrogen Energy 33 (2007) 889.
[10] C. San Marchi, D. K. Balch, K. Nibur, B. P. Somerday, J Pressure Vessel Technol 130 (2008) 041401.
[11] C. San Marchi, B. P. Somerday, X. Tang, G. H. Schiroky, Proceedings of PVP-2008: ASME Pressure Vessels and Piping Division Conference, Chicago IL, ASME, PVP2008-61240.
[12] C. San Marchi, T. Michler, K. A. Nibur, B. P. Somerday, Int J Hydrogen Energy 35 (2010) 9736.
[13] K. H. Lo, C. H. Shek, J. K. L. Lai, Materials Science and Engineering R 65 (2009) 39.
[14] D. Peckner, I. M. Bernstein, (Eds.). Handbook of Stainless Steels. New York: McGraw-Hill, 1977.
[15] J. Talonen, H. Hanninen, Acta Mater 55 (2007) 6108.
[16] T. S. Byun, Acta Mater 51 (2003) 3063.
[17] D. Hull, D. J. Bacon, Introduction to Dislocations, Butterworth Heinemann, Oxford UK, 1984.
[18] P. J. Ferreira, I. M. Robertson, H. K. Birnbaum, Acta Mater 47 (1999) 2991.
[19] G. Lu, Q. Zhang, N. Kioussis, E. Kaxiras, Physical Review Letters 87 (2001) 095501.
[20] I. M. Robertson, Eng Fract Mech 68 (2001) 671.
[21] J. P. Chateau, D. Delafosse, T. Magnin, Acta Mater 50 (2002) 1523.
[22] G. R. Caskey, in: Louthan MR, McNitt RP, (Eds.), Environmental Degradation of Engineering Materials, Virginia Polytechnic Institute, Blackburg VA, 1977, pp. 437.
[23] G. R. Caskey, Scr Metall 11 (1977) 1077.
[24] C. San Marchi, N. Y. C. Yang, T. J. Headley, J. Michael, 18th European Conference on Fracture (ECF18), Dresden, Germany, 30 August - 3 September 2010.
[25] Y. Tomota, Y. Xia, K. Inoue, Acta Mater 46 (1998) 1577.
[26] C. Liu, T. Hashida, H. Takahashi, H. Kuwona, Y. Hamaguchi, Metall Mater Trans 29A (1998) 791.
[27] D. G. Ulmer, C. J. Altstetter, Acta Metall Mater 39 (1991) 1237.
[28] D. P. Abraham, C. J. Altstetter, Metall Mater Trans 26A (1995) 2859.
[29] K. A. Nibur, D. F. Bahr, B. P. Somerday, Acta Mater 54 (2006) 2677.
[30] K. A. Nibur, B. P. Somerday, D. K. Balch, C. San Marchi, Acta Mater 57 (2009) 3795.
[31] C. San Marchi, K. A. Nibur, D. K. Balch, B. P. Somerday, X. Tang, G. H. Schiroky, T. Michler, in: Somerday BP, Sofronis P, Jones R, (Eds.), Effects of Hydrogen on Materials, ASM International, Materials Park OH, 2009, pp. 88.
[32] H. E. Hanninen, Inernational Metals Reviews 24 (1979) 85.

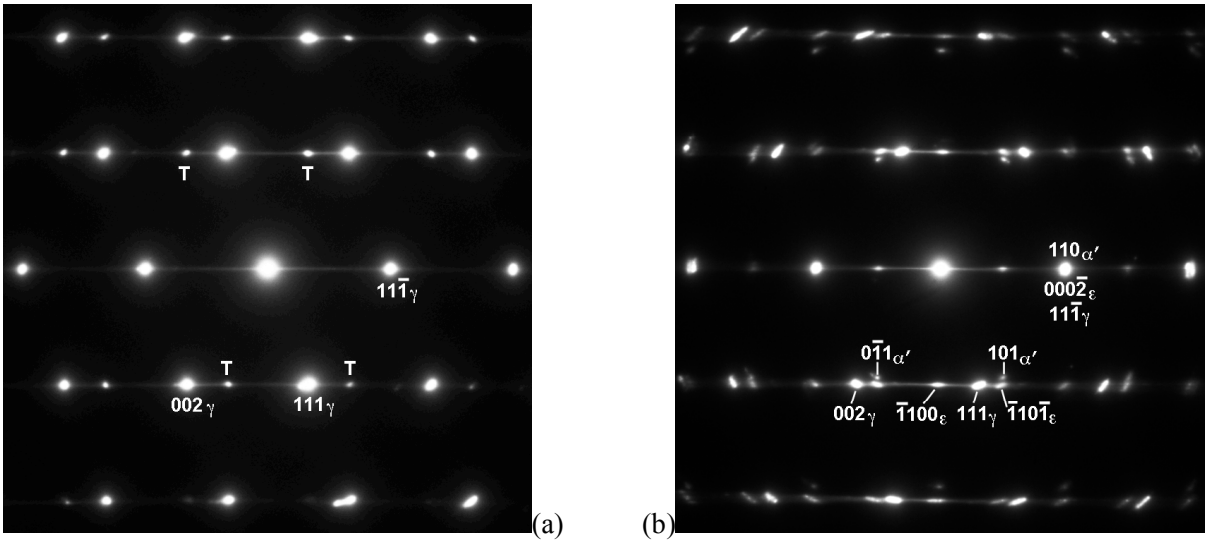

(a) (b)

Figure 1. SAED patterns of type 316L austenitic stainless steel: (a) deformed without hydrogen and (b) deformed with internal hydrogen (hydrogen-precharged in gaseous hydrogen at 300˚C, resulting in 0.7 at% hydrogen). T represents twinning reflection in γ, while in (b) the [-110]γ, [11-20]ε, and [-111] α' zone axes are superimposed.

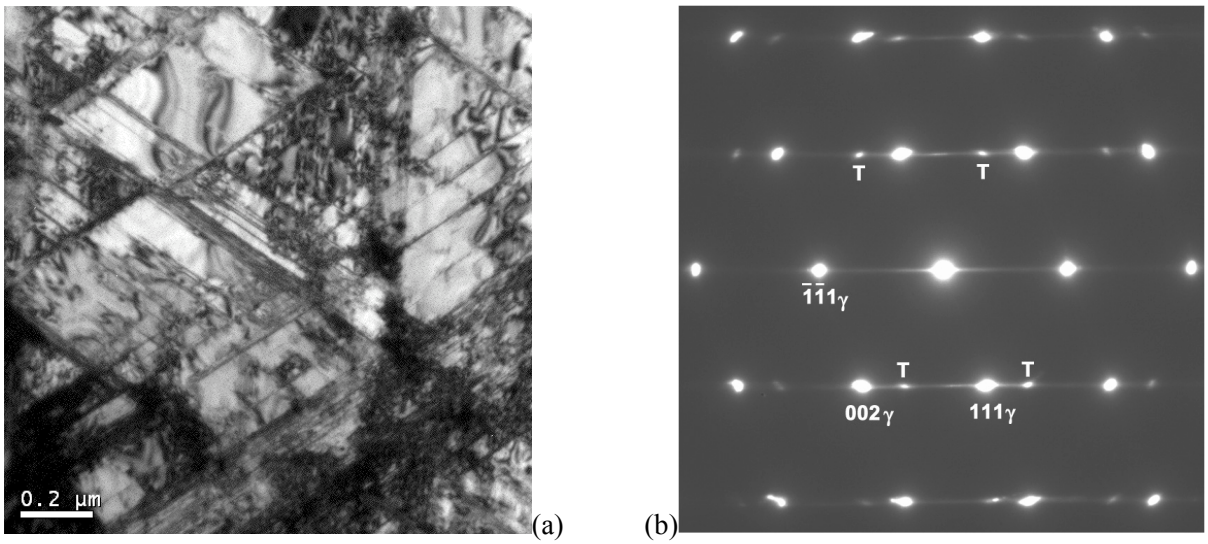

(a) (b)

Figure 2. Austenitic stainless steel 21-6-9 deformed to a strain of approximately 40% at 223 K in the non-charged condition. (a) TEM image showing high density of thin (111) deformation twins. (b) Typical SAED pattern showing deformation twin reflections (T).

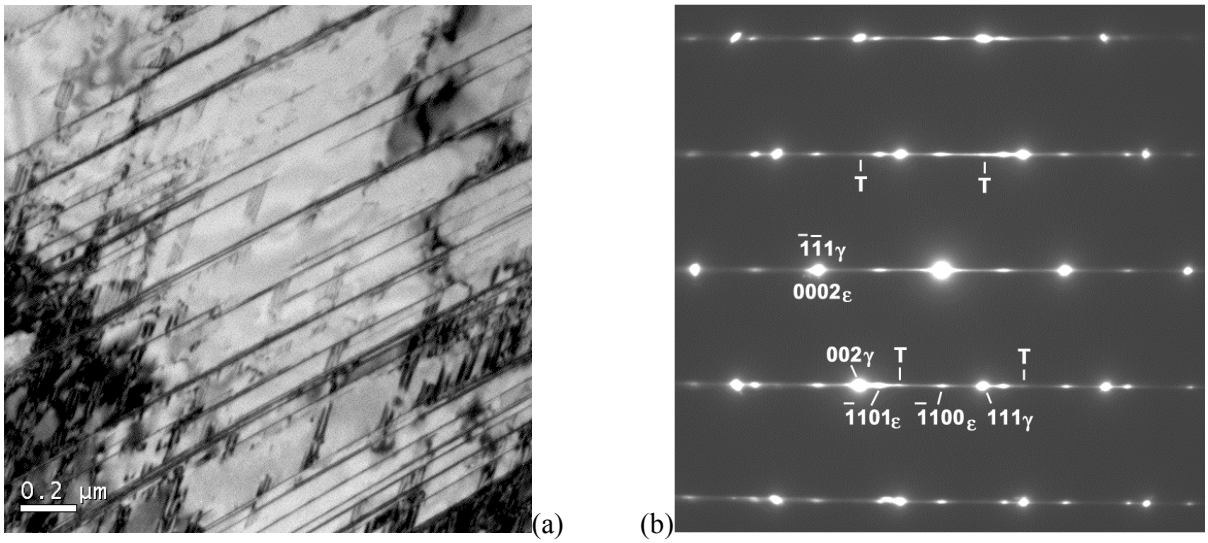

(a) (b)

Figure 3. Austenitic stainless steel 21-6-9 deformed to a strain of approximately 30% at 223 K in the hydrogen-precharged condition. (a) TEM image showing high density of thin ε-martensite platelets. (b) Typical SAED pattern confirming presence of ε-martensite and showing comparatively lower density of twin reflections (T) compared to deformation in the absence of hydrogen precharging.

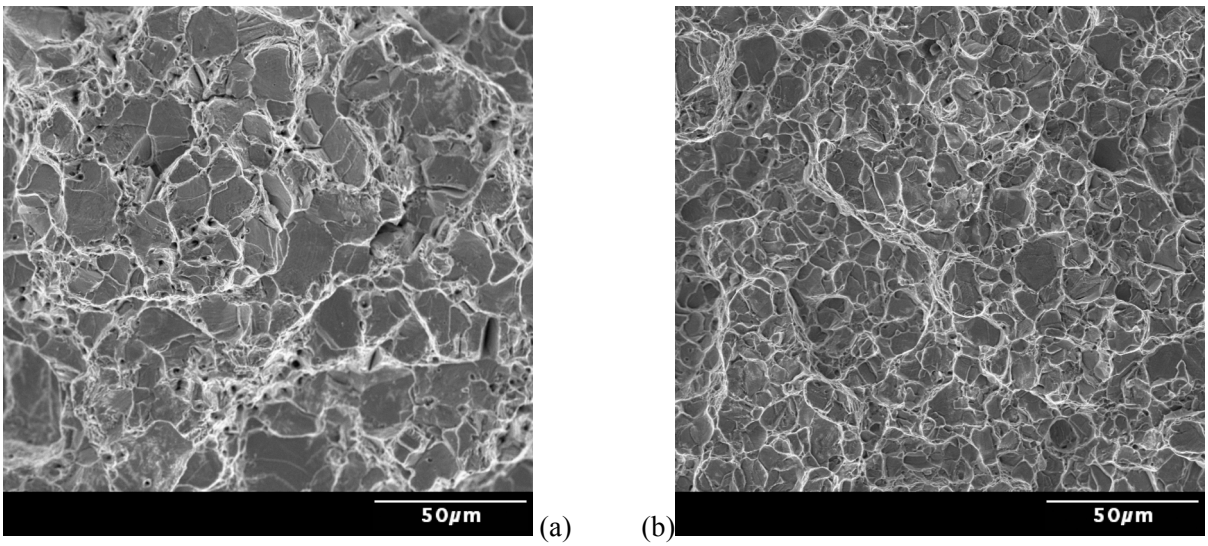

(a) (b)

Figure 4. Fracture surfaces of materials tested at temperature of 223 K after hydrogen-precharging: SEM images of (a) type 316L and (b) 21-6-9.